Published in final edited form as:
Circulation. 2014 September 30; 130(14): 1179–1191. doi:10.1161/CIRCULATIONAHA.113.007822.

The ERG-APLNR Axis Controls Pulmonary Venule Endothelial Proliferation in Pulmonary Veno-Occlusive Disease

Christopher Lathen, B.A.[1,*], **Yu Zhang, M.D., Ph.D.**[1,*], **Jennifer Chow**[1], **Martanday Singh, M.D.**[1], **Grace Lin, M.D., Ph.D.**[2], **Vishal Nigam, M.D., Ph.D.**[3], **Yasser A. Ashraf, M.D**[1], **Jason X. Yuan, M.D., Ph.D.**[4], **Ivan M. Robbins, M.D.**[5], and **Patricia A. Thistlethwaite, M.D., Ph.D.**[1,*]

[1]Division of Cardiothoracic Surgery, University of California, San Diego, CA

[2]Division of Pathology, University of California, San Diego, CA

[3]Division of Cardiology, University of California, San Diego, CA

[4]Department of Medicine, University of Illinois, Chicago, IL

[5]Division of Pulmonary Medicine, Vanderbilt University School of Medicine, Nashville, TN

Abstract

Background—Pulmonary veno-occlusive disease (PVOD) is caused by excessive cell proliferation and fibrosis which obliterates the lumen of pulmonary venules, leading to pulmonary hypertension, right ventricular failure, and death. This condition has no effective treatment and a 5-year survival of less than 5%. Understanding the mechanism of this disease and designing effective therapies is urgently needed.

Methods and Results—We show that mice with homozygous deletion of the Ets transcription factor, *Erg*, die between E16.5 and three months of age from PVOD, capillary hemorrhage, and pancytopenia. We demonstrate that Erg binds to and serves as a transcriptional activator of the G-protein-coupled receptor gene, *Aplnr*, whose expression in the vasculature is uniquely specific for venous endothelium, and that knockout of either *Erg* or *Aplnr* results in pulmonary venous-specific endothelial proliferation *in vitro*. We show that mice with either homozygous-global or endothelial-directed deletion of *Aplnr* manifest PVOD and right heart failure, detectable at 8 months of age. Levels of pulmonary ERG and APLNR in patients with PVOD undergoing lung transplantation were significantly lower than those of controls.

Conclusions—Our results suggest that ERG and APLNR are essential for endothelial homeostasis in venules in the lung and that perturbation in ERG-APLNR signaling is crucial for the development of PVOD. We identify this pathway as a potential therapeutic target for the treatment of this incurable disease.

Keywords

pulmonary hypertension; pulmonary veno-occlusive disease; pulmonary vascular remodeling

Correspondence: Patricia A. Thistlethwaite, MD, PhD, Division of Cardiothoracic Surgery, University of California, San Diego, 9300 Gilman Drive, MC 8892, San Diego, CA 92037, Phone: 858-657-7777, Fax: 858-657-5058, pthistlethwaite@ucsd.edu.
*contributed equally

Conflict of Interest Disclosures: None.

Introduction

Pulmonary veno-occlusive disease (PVOD) is characterized by structural remodeling of post-capillary venules and small veins in the lung, resulting in intimal thickening, fibrosis, luminal occlusion, and thrombosis. This disease is unique to the venous side of the pulmonary circulation, sparing the pulmonary arterial and systemic circulations. Clinically, PVOD results in progressive elevation in pulmonary arterial pressure, leading to right heart failure and death. PVOD is distinct from pulmonary arterial hypertension (PAH), a disease characterized by small pulmonary artery occlusion. PVOD accounts for 5–10% of unexplained pulmonary hypertension cases, and the median survival of PVOD patients is <3 years from diagnosis[1]. There is no effective therapy for PVOD, and lung transplantation is reserved for patients with end-stage disease. Critical barriers to designing PVOD therapies are the paucity of research focusing on the venous pulmonary circulation, the lack of animal models recapitulating this disease, and the absence of tools that allow for early diagnosis and the study of disease progression in humans.

Recently, Erg, a member of the Ets-family of transcription factors, has been identified as a key modulator of endothelial cell differentiation[2] and hematopoiesis[3]. Erg is required for angioblast differentiation along the endothelial/hematopoietic lineages, and is known to modulate endothelial-specific genes including *VE-cadherin (Cdh5), von Willebrand factor (Vwf), endoglin (Eng), intercellular adhesion molecule-2 (Icam2), secreted acidic cysteine rich glycoprotein (Sparc), angiopoietin-2 (Angpt2), EGF-like domain 7(Egfl7), endothelial nitric oxide synthase (Nos3), heme oxygenase (Hmox1), and hairy/enhancer-of-split 2* (*Hey2)*[2]. Suppression of Erg has been associated with decreased ability to form tube-like structures[4], and activation of proinflammatory genes, such as *interleukin 8* (*Il8)* and *nuclear factor of kappa light polypeptide gene enhancer in B-cells* (*Nfkb1)*[5,6]. Clues as to the role of Erg in endothelium have been suggested by experiments in *Xenopus*. Erg expression in embryos by RNA microinjection induces ectopic venous endothelial terminal differentiation and clustering, with cells expressing the transcript for *X-msr*, the homolog of the human *APLNR* gene[7].

Several lines of evidence suggest that the G protein-coupled receptor, APNR, functions in both the cardiac and vascular systems. Administration of apelin, the only known ligand for the Aplnr receptor, has been shown to increase cardiac contractility in animals[8], while left ventricular failure in humans is associated with low levels of apelin[9]. In addition to cardiac effects, a role for APNLR, is emerging in the venous vasculature. First, in the retinal vasculature of the mouse, Aplnr has been shown to be specific for venule endothelium[10]. Second, apelin has been found to have venodilator effects in conscious rats[11]. Third, apelin has been demonstrated to be a potent mitogenic and chemotactic factor in *in vivo* venous angiogenesis assays, involving *Xenopus* embryos and chicken chorioallantoic membrane[12]. Fourth, *apelin* or *Aplnr* knockdown inhibits hypoxia-induced venous regeneration in caudal fin regrowth of Fli-1 transgenic zebrafish[13]. These studies point to the concept that Aplnr signaling has direct and unique effects on the venous circulation.

With this background, we explored the role of Erg and Aplnr in the pulmonary venous circulation. We report the development of *Erg*- and *Aplnr*-null mice, as the first animal models for PVOD. We demonstrate a novel role of ERG signaling in controlling venous endothelial proliferation and show a mechanistic link through ERG-dependent activation of APLNR as critical to maintaining pulmonary venous endothelial homeostasis. Our work suggests that PVOD is caused by perturbations in the ERG-APLNR signaling pathway and provides a new therapeutic target for this lethal disease, with high translational potential.

Methods

A description of routine methodologies is provided in the Online Data Supplement.

Human tissue processing

Measurement of human pulmonary and systemic arterial pressures and lung biopsy were performed as previously described[14]. Tissue was collected from 15 human subjects with PVOD (systolic PAP > 90 mmHg, PVR > 680 dynes $sec^{-1}cm^{-5}$) undergoing lung transplantation and 15 individuals without pulmonary hypertension (mean PAP < 20 mmHg, PVR < 220 dynes $sec^{-1}cm^{-5}$) undergoing lung resection for benign nodules. PVOD or benign pathology was verified from explanted lung tissue by a pathologist. All subjects had given consent for lung biopsy. This study was approved by the UCSD Institutional Review Board, and experiments were performed within relevant guidelines and regulations of this body.

Generation of *Erg* and *Aplnr* Knockout Mice

Please refer to the Online Data Supplement.

Histologic and immuhistochemical analyses

Please refer to the Online Data Supplement.

Chromatin immunoprecipitation assay

Chromatin immunoprecipitation (ChIP) was performed using the Farnham Lab ChIPs protocol (Farnham Lab, Sacramento, CA). Mouse lung tissue was minced in cell lysis buffer containing protease inhibitor (Sigma, St. Louis, MO). After homogenizing at 4°C, genomic DNA was sheared by sonication into 1–2 kb fragments. Samples were centrifuged at 14,000 rpm for 10 minutes and the supernatant was divided evenly into four tubes. DNA extracted from the first aliquot was used as the total INPUT DNA. 2 μg Erg antibody and 2 μg of negative control IgG (rabbit) were added to the second and third aliquots respectively, and incubated overnight at 4°C. No antibody or IgG was added to the fourth aliquot, which was used as a negative control. Aliquots 2, 3, and 4 were incubated with Protein G beads for 1.5 hours. At the end of incubation, beads were washed, and immunoprecipitated DNA eluted and purified by reversing cross-linking, removal of RNA, and treatment with Proteinase K. Extracted DNA was used as template for qPCR using primers specific to the *Aplnr* promoter sequence in order to amplify regions containing putative ETS-binding sites. Primer sequences used are described in the Online Data Supplement.

RNA and protein methods

Please refer to the Online Data Supplement.

Measurement of luciferase activity

Please refer to the Online Data Supplement.

Isolation and culture of human and mouse pulmonary venous endothelial cells (PVECs) and pulmonary artery endothelial cells (PAECs)

Please refer to the Online Data Supplement.

Endothelial cell growth assays and adenoviral transduction

Human PVECs or mouse PVECs derived from the lungs of 5 $Erg^{-/-}$ and 5 $Erg^{+/+}$ mice were used for endothelial cell growth assays. Cells were seeded at 5×10^5 cells per 35 mm diameter well and 12 hours later, growth-arrested by washing the cells three times with PBS prior to the addition of endothelial cell growth media (Cell Application, Inc.) without fetal bovine serum. Cells were incubated at 37° C, 5% CO_2 for 6 hours and then treated with adenovirus (pAd/CMV/V5-DEST vector [Invitrogen] containing the cytomegalovirus [CMV] early promoter driving either mouse *Erg*, human *ERG*, or mouse *Aplnr* [amino acid sequences for Erg and Aplnr vectors in the Online Data Supplement]). Adeno-*Erg*, Adeno-*ERG*, and Adeno-*Aplnr* vectors also contained the *Escherichia coli* lacZ gene driven by a second CMV early promoter. Transduction efficiency was assessed by measuring the ratio of X-gal-stained cells to non-stained cells for each vector transduction. For all vectors, 12 independent viral infections per subculture were performed, with a multiplicity of infection = 100. Cell counts and ^{3}[H]leucine incorporation assays were performed as previously described[14].

Apelin measurements

Please refer to the Online Data Supplement.

Mouse hemodynamic measurements, pulmonary angiography, and cardiovascular evaluation

Animal experiments were approved by the UCSD Animal Subjects Committee and were done in accordance with the relevant guidelines of the NIH Guide for the Care and Use of Laboratory Animals. We performed mouse hemodynamic measurements, pulmonary arteriography, and cardiac weight studies as previously described[14]. For retrograde pulmonary venous angiography, animals were sacrificed and left thoracotomy with pericardiectomy was performed. The main pulmonary artery was divided, allowing for free egress of blood from the pulmonary artery. The left superior pulmonary vein was cannulated with a 29-gauge needle and the left upper lobe was perfused *in situ* through the left superior pulmonary vein with 3 ml of Microfil, a liquid silicon-based polymer (Flow-tech, Carver, MA), for 1 minute using an infusion pump. For coronary angiography, animals were sacrificed, a cross-clamp placed on the ascending aorta, and the coronaries perfused with 1 ml of Microfil, for 1 minute using an infusion pump. For pulmonary arteriography, pulmonary venography, and coronary angiography, Microfil was allowed to harden *in situ*

for approximately 1 hour. Organs were harvested, processed per the manufacturer's protocol, and photographed using a digital photomicroscope (Zeiss, Jena, Germany).

Epoprostenol-challenge and pulmonary vein contraction experiments

Please refer to the Online Data Supplement.

Echocardiographic assessment of cardiac function

Please refer to the Online Data Supplement.

Statistical analysis

Data are expressed as mean ± s.e.m. Statistical analysis was carried out using the Kruskal-Wallis one-way ANOVA for multiple group analysis. When two groups with continuous data were compared, statistical differences were assessed with the Wilcoxon rank sum test. All *P*-values are two-sided, with significance defined as $P < 0.01$. Due to the nature of the study, there was no adjustment for multiple comparisons. The number of animals/samples in each group is indicated in the figure legends or methods.

Results

Vascular expression of Erg and Aplnr

We studied the expression of the transcription factor, ERG, in human and mouse heart and lung. Immunofluorescent staining showed ERG expression was confined to nuclei of cardiomyocytes in the outer myocardium as well as endothelial cells in arteries and veins of the pulmonary and coronary circulations in humans and mice (Fig. 1A). Since *X-msr (Aplnr)* had been implicated as a target of Erg in *Xenopus* and to facilitate visualization of Aplnr expression, we generated *nlacZ* (*nuclear lacZ*) knock-in into the endogenous *Aplnr* locus in mouse (Fig. S1). We found that nlacZ expression was confined to cardiomyocytes as well as venous endothelium in all organs tested (Fig. 1, B–D, Fig. S2). Co-immunostaining with Pecam-1, Neuropilin-1 (Nrp-1: artery endothelial-specific), and Nuclear receptor subfamily 2 group F member (Nr2f-2: known as COUPTF-II: vein endothelial-specific) antibodies confirmed that β-gal (Aplnr) expression localized to venous endothelium, while Erg expression localized to arterial and venous endothelium in the lungs and heart (Fig. 1, C–E, Fig. S2). We further showed that Aplnr expression is not seen in lymphatic vessels, by performing co-immunostaining experiments with monoclonal antibody to podoplanin, a lymphatic endothelial marker in mice[15], in conjunction with antibody to β-gal (Aplnr). Podoplanin expression was isolated to lymphatic vessels in mouse lung, while Aplnr expression was confined to veins only (data not shown).

Erg binds to the *Aplnr* promoter, activating *Aplnr* transcription in pulmonary venous enodothelial cells

We identified that the mouse and human *Aplnr* promoters (−3179 to −1) each contain 12 Erg binding sites, identified by the consensus sequence (A/G)(G/C)AGGAA(A/G)[6]. Chromatin immunoprecipitation (ChIP) assays showed that Erg binds to the mouse *Aplnr* promoter,

with strong affinity of Erg to the consensus site located at 248 base pairs proximal to the *Aplnr* transcription start site (Fig. 2, A–B).

We investigated whether ERG overexpression was associated with increase of *APLNR* mRNA *in vitro*. Human pulmonary venous endothelial cells (PVECs isolated from pulmonary veins <500μm diameter) and human pulmonary arterial endothelial cells (PAECs isolated from pulmonary arteries <500μm diameter) infected with *ERG* adenovirus showed constitutive ERG protein levels compared to *lacZ*-transduced cells (Fig. 2C). PVECs transduced with ERG adenovirus showed markedly higher levels of *APLNR* mRNA compared to PAECs transduced with the same vector and *lacZ*-transduced cells (Fig. 2D–E). Selective induction was seen for *APLNR* expression in PVECs and not for other genes known to be transcriptionally-activated by ERG, including *CDH5*, *HMOX1*, *HEY2*, and *ICAM2* (Fig. 2F). Using a dual-luciferase reporter assay, we found strong activation of *APLNR* transcription in the presence of ERG in human PVECs, but not in human PAECs (Fig. 2G). Progressive deletion of the promoter region of *APLNR* in luciferase assays demonstrated that region −600 to −200 was necessary for promoter activity in the presence of ERG in PVECs (Fig. 2H). These results suggest that ERG regulates *APLNR* expression through a promoter-dependent mechanism in pulmonary venous endothelium.

High level ERG expression in human PVECs conferred a significantly decreased growth rate at preconfluence and decreased proliferation, as determined by ^{3}[H]leucine incorporation (Fig. 2I). Constitutive ERG expression in PAECs did not affect growth rate or proliferation (Fig. 2I). Apelin12 levels in culture supernatants were equal in *ERG* and *lacZ*-transduced PVECs and PAECs (*ERG*-transduced PVECs: 0.07±0.04ng/ml; *lacZ*-transduced PVECs: 0.09±0.05ng/ml; *ERG*-transduced PAECs: 0.07±0.06ng/ml; *ERG*-transduced PAECs: 0.08±0.05ng/ml). There was no difference in apelin protein levels in human PVECs and PAECs transduced with either *ERG* or *lacZ* by Western blotting.

Decreased ERG and APLNR correlate with PVOD phenotype in humans

We examined the expression pattern of ERG and APLNR in the lungs of 15 PVOD patients and compared them to lung biopsies from 15 individuals without pulmonary hypertension. We found significantly decreased levels of ERG protein (Fig. 3A) and *APLNR* mRNA and protein (Fig. 3B, C) in human PVOD lung tissue compared to normotensive controls. In contrast, we found no difference in the levels of other genes controlled by ERG (*CDH5*, *NOS3*, *HMOX1*, *HEY2*, and *ICAM2*) in PVOD specimens compared to controls (Fig. 3D). These results suggest that attenuation of ERG and APLNR correlate with the PVOD disease phenotype in humans.

Erg$^{-/-}$ mice develop lethal PVOD

To test whether diminished Erg expression causes PVOD, we generated a knockout mouse with cre-mediated deletion of *Erg* (Fig. S3, A–C). Heterozygous animals appeared phenotypically normal. In *Erg*$^{-/-}$ mice, lethality occurred between E16.5 and 3-months with 100% penetrance (Fig. S3, D–E). *Erg*$^{-/-}$ mice had no detectable Erg protein in lung tissue by Western blotting, indicating that postnatal survival was not linked to fidelity of gene knockout (Fig. S3, C).

Erg$^{-/-}$ mice demonstrated occlusion and luminal narrowing of postcapillary pulmonary venules (<250μm diameter) (Fig. 4A), pancytopenia (Table S1), and variable pulmonary capillary hemorrhage (Fig. 4B). Elastic-Van Gieson staining (Fig. 4A), immunostaining with antibody to Nr2f-2, and lack of immunostaining with antibody to Nrp-1, verified that occluded vessels were venules (Fig. 4C). Cells blocking venule lumina in the pulmonary circulation stained positive for Pecam-1, but not Acta-2, indicating endothelial phenotype (Fig. 4C). Small pulmonary arteries were histologically normal (Fig. 4A). Morphometric studies of lungs from *Erg*$^{-/-}$ mice were performed to assess evidence of post-capillary venule remodeling. Pulmonary venule occlusion was widespread in *Erg*-null mice and not seen in littermate controls (Table S2). Venule intimal thickening correlated with cellular proliferation as measured by the number of cells positively stained for PCNA in *Erg*$^{-/-}$ mice (Fig. 4A, Table S2). Vessel/alveoli ratios were not significantly different between *Erg*$^{-/-}$ mice and littermate controls (Table S2). Apoptotic cells were not detected in pulmonary venules in *Erg*$^{-/-}$ or *Erg*$^{+/+}$ mice by TUNEL assay, suggesting that decreased apoptosis was not contributing to vessel occlusion.

Postnatal *Erg*$^{-/-}$ mice developed markedly elevated right ventricular systolic pressures (RSVP) (39±2mmHg at four weeks to 50±5mmHg at eight weeks) (Fig. 4D). Venous angiograms of *Erg*$^{-/-}$ mice were markedly abnormal with small-vessel pruning and absence of peripheral vascular blush, while pulmonary arteriograms were normal-appearing (Fig. 4E). We confirmed the presence of pulmonary hypertension from venous obstruction in *Erg*$^{-/-}$ mice that survived past 4 weeks by measurement of right ventricular hypertrophy. The ratio of RV weight to that of the left ventricle and septum was significantly increased in 4-week old *Erg*$^{-/-}$ mice, compared to that seen in heterozygous and wildtype littermates (Fig. 4F). *Erg*$^{-/-}$ mice challenged with the pulmonary vasodilator, epoprostenol, developed life-threatening pulmonary edema, similar to the response of this drug in humans with PVOD (Fig. 4G). Vasodilator-induced pulmonary edema in humans with PVOD results from vasodilation of the pre-capillary vessels more so than post-capillary vessels, leading to increases in trans-capillary hydrostatic pressure and fluid transudation into alveolar spaces[16].

To test whether RV failure was due to PVOD rather than coronary defects, we performed coronary arteriography and venous photography in *Erg*$^{-/-}$ mice and littermates. No difference was noted in coronary artery/vein configuration or luminal diameter between null animals and littermates (Fig. 4H). Coronary arteries and veins in *Erg*$^{-/-}$ mice were histologically normal-appearing. To ascertain if there were effects of *Erg* knockout on left heart function, we performed echocardiography on 4-week old *Erg*$^{-/-}$ and control mice. *Erg*$^{-/-}$ mice had normal left ventricular systolic function, thickness, inner diameter, and fractional shortening similar to that seen in wildtype animals (Table S3).

Erg inhibits proliferation of pulmonary venous endothelial cells through Aplnr

As endothelial proliferation is a mechanism of vascular remodeling in PVOD, we investigated whether homozygous deletion of *Erg* affected PVEC proliferation through modulation of *Aplnr*. First, we found that within *Erg*$^{-/-}$ mouse lungs, there were undetectable *Aplnr* mRNA levels (Fig. 5A). *Erg*$^{-/-}$ PVECs had markedly diminished

expression *Aplnr* mRNA compared to wildtype PVECs (Fig. 5B). Second, growth rates of $Erg^{-/-}$ and $Aplnr^{-/-}$ PVECs were compared to wildtype PVECs. Knockout of *Erg* (Fig. 5C) or *Aplnr* (Fig. 5D) in PVECs resulted in significantly increased growth rates at preconfluence and increased proliferation, as determined by ^{3}[H]leucine incorporation, compared to wildtype PVECs. In contrast, knockout of *Erg* (Fig. 5C) or *Aplnr* (Fig. 5D) in PAECs had no measurable effect on PAEC growth rate, proliferation, or ^{3}[H]leucine incorporation. These data suggested that the normal function of the Erg-Aplnr axis in PVECs is to limit proliferation and maintain cellular quiescence. We performed rescue experiments to determine whether repletion of Erg or Aplnr in $Erg^{-/-}$ PVECs would attenuate PVEC proliferation. Constitutive expression of *Erg* in $Erg^{-/-}$ PVECs restored high levels of *Aplnr* expression (Fig. 5E) and decreased cellular proliferation and ^{3}[H]leucine incorporation (Fig. 5F). *Aplnr* overexpression in $Erg^{-/-}$ PVECs transduced with an *Aplnr* adenovirus independently diminished proliferation and ^{3}[H]leucine incorporation in $Erg^{-/-}$ cells (Fig. 5G).

Aplnr null mice develop late PVOD

To understand the role of Aplnr in the pulmonary venous vasculature, we studied mice with a global (*$Aplnr^{-/-}$:nlacZ*) or endothelial-directed *($Aplnr^{flox/flox}$:nlacZ*-Flk-1Cre, abbreviated as: *$Aplnr^{f/f}$:nlacZ*-Flk-1Cre) knockout of *Aplnr* (Fig. S1). *$Aplnr^{-/-}$:nlacZ* and *$Aplnr^{f/f}$:nlacZ*-Flk-1Cre mice were born alive with normal Mendelian ratios, without obvious vascular abnormality. However, by eight months of age, both sets of *Aplnr* null animals developed elevation of pulmonary pressures under ambient oxygen conditions (Fig. 6A). Lungs from *$Aplnr^{-/-}$:nlacZ* mice showed normal pulmonary arterial anatomy, distribution, and patency; however, pulmonary venules (<250μm diameter) in all lobes manifest narrowing and occlusion, similar to the phenotype seen in $Erg^{-/-}$ mice (Fig. 6B). Cells blocking venule lumina stained positive for Pecam-1 and Nr2f-2, and negative for Nrp-1 and Acta-2 indicating venous endothelial phenotype (Fig. 6C). Pulmonary hemorrhage was not seen. PCNA expression was higher in small venules in *Aplnr* null mice compared to littermates at 8 months (Fig. 6B). Quantification revealed more than 60% of pulmonary venules were occluded in *$Aplnr^{-/-}$:nlacZ* and *$Aplnr^{f/f}$:nlacZ*-Flk-1Cre mice, while vessel/alveoli ratios were similar between knockout and control mice at 10 months (Table S4).

Pulmonary venograms of 10-month old *$Aplnr^{-/-}$:nlacZ* and *$Aplnr^{f/f}$:nlacZ:*-Flk-1Cre PVOD mice, displayed vessel blunting and absence of peripheral blush; whereas, control littermates had pulmonary venograms with normal vascular filling (Fig. 6D). *$Aplnr^{-/-}$:nlacZ* and *$Aplnr^{f/f}$nlacZ*-Flk-1Cre mice had normal-appearing pulmonary arteriograms (Fig. 6D).

At 8–10 months of age, *$Aplnr^{-/-}$:nlacZ* and *$Aplnr^{f/f}$:nlacZ*-Flk-1Cre mice both showed evidence of RV hypertrophy by chamber weight and size (Fig. 6E). Vasodilator challenge of 10-month old *$Aplnr^{-/-}$:nlacZ and $Aplnr^{f/f}$nlacZ*-Flk-1Cre mice with epoprostenol, induced development of severe pulmonary edema, similar to the response of this drug in $Erg^{-/-}$ mice (Fig. 6F).

Based on data suggesting that apelin may function as a systemic venodilator in rats[11], we examined whether pulmonary hypertension in *Aplnr* null mice could be attributed to alterations in pulmonary venous myogenic tone. We compared agonist-mediated

vasoconstriction of isolated intrapulmonary small veins from *Aplnr*$^{-/-}$*:nlacZ* mice and wild-type littermates. The active tension induced by high K^+ or U-46619 (thromboxane A_2 analogue) treatment of vein rings was not significantly different between *Aplnr*$^{-/-}$*:nlacZ* and *Aplnr*$^{+/+}$*:nlacZ* mice (Fig. S4). We also tested whether there is a venodilator effect of apelin on pulmonary vessels in wildtype mice. We found that 0.1μM–100μM apelin had no effect on active tension induced by phenylephrine in pulmonary vein rings derived from wildtype mice, suggesting differences in the effect of apelin on systemic and pulmonary circulations (Fig. S5).

We examined whether global or endothelial-specific *Aplnr* knockdown affected myocardial performance. Echocardiograms of 8 to 10-month old *Aplnr*$^{-/-}$*:nlacZ and Aplnr*$^{f/f}$*:nlacZ-*Flk-1Cre mice demonstrated normal left ventricular dimensions, wall thickness, and fractional shortening (Table S5). Coronary artery and vein anatomy and size did not differ between *Aplnr*$^{-/-}$ mice and controls (Fig. 6G). Collectively, this data suggests that *Aplnr* knockout did not have a direct effect on myocardial function, and that the development of RV hypertrophy correlated with development of PVOD and pulmonary hypertension.

Discussion

The identification of pathways that regulate venous endothelium and the possibility of manipulating such pathways *in vivo* have potential therapeutic applications. This study identifies ERG and APLNR as crucial mediators of PVEC proliferation and crucial mediators for the development of rodent PVOD and possibly human PVOD.

Our goal has been to understand the molecular causes of different types of human pulmonary hypertension, and in doing so shed light on the fundamental differences between arteries and veins. From the work presented, we have four major conclusions. First, we show that Aplnr is specific for venous endothelium in multiple organs in both mice and humans. This result underscores that the physiological and pathological distinctions between arteries and veins are not due simply to differences in anatomy, oxygenation, or blood pressure, but are related to a specific genetic difference. Second, we show that the transcription factor, ERG, regulates venous-specific *APLNR* expression in mice and humans. In previous studies, Erg has been necessary for self-renewing hematopoiesis and marrow angioblast differentiation in the embryo[17]. Our findings of PVOD and pancytopenia in *Erg*$^{-/-}$ mice raise the question whether venous specificity through the Erg-Aplnr axis may occur before separation of hematopoietic and endothelial lineages. Third, we find that the anatomic consequence of *Erg* or *Aplnr* knockout is the development of PVOD, with small pulmonary venule occlusion secondary to excessive endothelial proliferation. This finding, coupled with the observation that ERG and APLNR are markedly diminished in lungs of individuals with PVOD, support a role of ERG and APLNR in modulating venous endothelial homeostasis within the pulmonary vasculature. Although vasodilator effects have been reported for apelin in the systemic circulation[11], we found no evidence that *Aplnr* knockout affects vasoreactivity of the pulmonary circulation. Similar to our data, others have shown that administration of apelin to normal anesthesized dogs has no effect on the mean pulmonary artery pressure[18]. Fourth, we demonstrate that absence of Erg expression in venous endothelium confers proliferative capacity on PVECs, and that restoration of either

Erg or *Aplnr* expression attenuates proliferation of venous endothelial cells *in vitro*. Collectively, these results suggest the normal function of the Erg-Aplnr axis is to suppress venous endothelial proliferation and maintain cellular quiescence within the adult lung.

Human PVOD has no known cure, except lung transplantation. To date, the processes that contribute to intimal hyperplasia and fibrosclerosis seen in venules and small veins within the lung of PVOD patients are unknown, although by pathologic and immnuohistochemical analysis, neointimal cells seen in PVOD have characteristics and biomarkers of endothelium[19]. We have chosen to focus on endothelial proliferation as a potential contributor to disease phenotype, although we recognize that other mechanisms, such as acute inflammation, peri-venular fibrosis, and cellular migration or transdifferentiation within the wall of pulmonary veins may also play a role.

Human PVOD may occur as an isolated entity or in conjunction with pulmonary capillary hemangiomatosis (PCH), a condition characterized by abundant well-circumscribed areas of capillary proliferation that expand alveolar septa and often invade bronchial walls and pleura[19]. To date, it is unknown whether PVOD and PCH are distinct disorders or different overlapping manifestations of the same disorder. Our $Erg^{-/-}$ and $Aplnr^{-/-}$ mice that develop PVOD do not manifest PCH pathology, and as such represent animal models for study of pure post-capillary venous obstructive pathology.

Clues as to why ERG may have a role in vessel narrowing/occlusion seen in PVOD may be analyzed from studies examining vessel caliber and lumen patency in zebrafish, *Xenopus*, and mice. Others have demonstrated Erg expression in areas of capillary-venous sprouting *in utero* and venules in the adult frog[10,12]. Erg has also been shown to control the expression of Egfl7, a secreted protein that regulates lumen formation in blood vessels in zebrafish[20] and inhibits Notch activity in murine endothelium[21]. Notch negatively regulates endothelial proliferation, where it inhibits endothelial cell sprouting responses. Loss of *Egfl7* in zebrafish blocks vascular tubulogenesis and attenuates luminal patency[20]. Thus, it is possible that Erg not only to limits proliferation of venous endothelium through transcriptional upregulation of *Aplnr*, but also through the modulation of *Egfl7* or *Notch*. The fact that $Erg^{-/-}$ mice develop pancytopenia and manifest lung hemorrhage with a more severe, earlier onset phenotype of PVOD than $Aplnr^{-/-}$ mice suggests that Erg may have effects on multiple pathways. Pulmonary capillary hemorrhage in $Erg^{-/-}$ PVOD mice correlates with earlier work showing that Erg is a positive regulator of *Cdh5* and *Icam2*[4], both genes encoding proteins which promote endothelial integrity. Occult pulmonary hemorrhage occurs often in humans displaying PVOD, previously thought to be solely due to post-capillary block[16].

In support of a role of Aplnr in vascular homeostasis, we provide evidence that Aplnr signaling is crucial for maintaining correct endothelial cell number that maintains luminal patency of venules in the lung. Our work contrasts with findings from others, that suggest apelin has effects in the adult rodent arterial circulation (where Aplnr is not expressed), including vasodilation[22], aneurysm formation[23], atherosclerosis enhancement[23], and protection against PAH[24]. The clearcut specificity of Aplnr for veins suggests that the

reported effects of apelin in arteries, may be due to interaction with a different receptor from Aplnr.

Currently, apelin is the only known ligand for Aplnr, and Aplnr is considered to be the only receptor for apelin. However, it is important to note that the phenotype of *Aplnr*$^{-/-}$ mice is different from that of *apelin*$^{-/-}$ mice[25]. Similarly, developmental work in zebrafish has suggested that the loss of *apelin* does not phenocopy the loss of *Aplnr* (*agtrl 1b*)[26]. The differences between *apelin* and *Aplnr* null mice, particularly with respect to PAH and PVOD, may reflect other unknown ligands and/or receptors, or ligand-independent functions of Aplnr, such as heterodimerization with other G protein-coupled receptors (GPCRs). In support of this concept is the observation that Aplnr and the GPCR angiotensin II type-1A receptor have been found to physically associate intracellularly, under certain conditions[23].

Our work underscores the concept that receptors and transcription factors may play different roles in different tissues. Previous studies have focused on the effects of apelin levels on cardiac contractility, with increased cardiac levels seen in RV hypertrophy and reduced levels seen in RV failure[27]. Although we find that in addition to venous endothelial expression, Aplnr is found in right and left ventricular cardiomyocytes, we have been unable to demonstrate any difference in left ventricular myocardial contractility between global and endothelial-directed *Aplnr* null mice and control littermates. We have found that ventricular size and function are normal in *Aplnr*$^{-/-}$*:nlacZ* and *Aplnr*$^{f/f}$*:nlacZ*-Flk-1Cre mice and that secondary RV hypertrophy and failure occur only after the development of PVOD. Taken together with our data, the observation that apelin may improve RV function in experimental models of PAH[28] suggests that either Aplnr signaling may improve pulmonary venous patency with consequent improvement in RV unloading, or apelin may have direct effects on the failing RV. We cannot exclude the possibility that RV failure in our *Aplnr*$^{-/-}$*:nlacZ* and *Aplnr*$^{f/f}$*:nlacZ*-Flk-1Cre mice is due to concurrent effects of PVOD leading to RV compromise and as yet unstudied gene effects on coronary venous function in a similar timeframe.

Finally, it has been suggested that PVOD is both a proliferative and inflammatory-fibrotic vasculopathy. The lung phenotype observed in *Erg* and *Aplnr* knockout mice demonstrates that intimal proliferation is a key component of pulmonary venule obstruction in these models of disease. Erg has also been found to have anti-inflammatory effects in endothelial cells *in vitro* through the repression of the *Il8* gene and inhibition of the TNF-α-dependent activation of *Nfkb1*[5,6]. Further studies will be necessary to assess whether diminished levels of Erg-Aplnr signaling seen in mouse and human PVOD affects inflammation and development in this vascular bed too.

In summary, our work shows that diminished or absent steady-state levels of ERG and APLNR are associated with the development of PVOD in humans and mice. Our results suggest that control of endothelial proliferation in post-capillary venules by Erg and Aplnr is a key process in venous endothelium homeostasis and may have important implications for the understanding of venous endothelial identity and the treatment of PVOD. Our work underscores the concept that the endothelium of the pulmonary venous circulation is functionally and genetically distinct from the pulmonary arterial circulation and provides a

framework for testing therapies for one of the most lethal diseases known to man. Augmentation of the expression or function of this pathway in the pulmonary vasculature may be a useful strategy to treat PVOD in humans.

Addendum

Since the submission of this manuscript, one group has reported that mutations in the gene, EIF2AK4, are associated with the development of familial PVOD and one quarter of non-familial PVOD cases[29], while another group has reported mutations in the same gene are associated with the development of familial PCH and one fifth of non-familial PCH cases[30]. We subsequently examined the expression of *Eif2ak4* in the lungs of our two animal models for PVOD. We found no difference in the expression of *Eif2ak4* in lung tissue from animals with homozygous or heterozygous deletion of *Erg* or *Aplnr* compared to the lungs of wildtype littermates by qRT-PCR (Fig. S6). Further studies will be needed to explore the role of Eif2ak4, a kinase known to phosphorylate the α subunit of eukaryotic translation initiation factor 2[31], with respect to Erg/Aplnr signaling.

Supplementary Material

Refer to Web version on PubMed Central for supplementary material.

Acknowledgments

Funding Sources: This work was supported by grants from the National Institutes of Health/National Heart, Lung, and Blood Institute (2R01HL70852 to P.A.T.) and (1P01 HL098053 to multiple investigators, including P.A.T.)

References

1. Montani D, Price LC, Dorfmuller P, Achouh L, Jais X, Yaici A, Sitbon O, Musset D, Simmoneau G, Humbert M. Pulmonary veno-occlusive disease. Eur Respir J. 2009; 33:189–200. [PubMed: 19118230]
2. Nikolova-Krstevski V, Yuan L, Bras AL, Vijayaraj P, Kondo M, Gebauer I, Bhasin M, Carman CV, Oettgen P. ERG is required for the differentiation of embryonic stem cells along the endothelial lineage. BMC Develop Biol. 2009; 9:72.
3. Loughran SJ, Kruse EA, Hacking DF, de Graaf CA, Hyland CD, Willson TA, Henley KJ, Ellis S, Voss AK, Metcalf D, Hilton DJ, Alexander WS, Kile BT. The transcription factor Erg is essential for definitive hematopoiesis and the function of adult hematopoietic stem cells. Nat Immunol. 2008; 9:810–819. [PubMed: 18500345]
4. McLaughlin F, Ludbrook VJ, Cox J, von Carlowitz I, Brown S, Randi AM. Combined genomic and antisense analysis reveals that the transcription factor Erg is implicated in endothelial differentiation. Blood. 2001; 98:3332–3339. [PubMed: 11719371]
5. Sperone A, Dryden NH, Birdsey GM, Madden L, Johns M, Evans PC, Mason JC, Haskard DO, Boyle JJ, Paleolog EM, Randi AM. The transcription factor Erg inhibits vascular inflammation by repressing NF-κB activation and proinflammatory gene expression in endothelial cells. Arterioscler Thromb Vasc Biol. 2011; 31:142–150. [PubMed: 20966395]
6. Yuan L, Nikolova-Krstevski V, Zhan Y, Kondo M, Bhasin M, Varghese L, Yano K, Carman CV, Aird WC, Oettgen P. Antiinflammatory effects of the ETS factor ERG in endothelial cells are mediated through transcriptional repression of the interleukin-8 gene. Circ Res. 2009; 104:1049–1057. [PubMed: 19359602]
7. Baltzinger M, Mager-Heckel AM, Remy P. X1erg: expression pattern and overexpression during development plead for a role in endothelial differentiation. Develop Dyn. 1999; 216:420–433.

8. Berry MF, Pirolli TJ, Jayasnakar V, Burdick J, Morine KJ, Gardner TJ, Woo WJ. Apelin has in vivo inotropic effects on normal and failing hearts. Circulation. 2004; 110:II187–193. [PubMed: 15364861]
9. Chong KS, Gardner RS, Morton JJ, Ashley EA, McDonagh TA. Plasma concentrations of the novel peptide apelin are decreased in patients with chronic heart failure. Eur J Heart Fail. 2006; 8:355–360. [PubMed: 16464638]
10. Saint-Geniez M, Argence CB, Knibiehler B, Audigier Y. The msr/apj gene encoding the apelin receptor is an early and specific marker of the venous phenotype in the retinal vasculature. Gene Exp Patt. 2003; 3:467–472.
11. Cheng X, Cheng XS, Pang CC. Venous dilator effect of apelin, an endogenous peptide ligand for the orphan APJ receptor, in conscious rats. Eur J Pharmacol. 2003; 470:171–175. [PubMed: 12798955]
12. Cox CM, D'Agostino SL, Miller MK, Hiemark RL, Krieg PA. Apelin, the ligand for the endothelial G-protein-coupled receptor, APJ, is a potent angiogenic factor required for normal vascular development in the frog embryo. Dev Biol. 2006; 296:177–189. [PubMed: 16750822]
13. Eyries M, Siegfried G, Ciumas M, Montagne K, Agrapart M, Lebrin F, Soubrier F. Hypoxia-induced apelin expression regulates endothelial cell proliferation and regenerative angiogenesis. Circ Res. 2008; 103:432–440. [PubMed: 18617693]
14. Li X, Zhang X, Leathers R, Makino A, Huang C, Parsa P, Macias J, Yuan JX-Y, Jamieson SW, Thistlethwaite PA. Notch3 signaling promotes the development of pulmonary arterial hypertension. Nat Med. 2009; 15:1289–1297. [PubMed: 19855400]
15. Schacht V, Dadras SS, Johnson LA, Jackson DG, Hong YK, Detmar M. Up-regulation of the lymphatic marker podoplanin, a mucin-type transmembrane glycoprotein, in human squamous cell carcinomas and germ cell tumors. Am J Pathol. 2005; 166:913–921. [PubMed: 15743802]
16. Montani D, Jais X, Dorfmuller P, Simmoneau G, Sitbon O, Humbert M. Goal-oriented therapy in pulmonary veno-occlusive disease: a word of caution. Eur Respir J. 2009; 34:1204–1206. [PubMed: 19880623]
17. Taoudi S, Bee T, Hilton A, Knezevic K, Scott J, Willson TA, Collin C, Thomas T, Voss AK, Kile BT, Alexander WS, Pimanda JE, Hilton DJ. Erg dependence distinguishes developmental control of hematopoietic stem cell maintenance from hematopoietic specification. Genes Dev. 2011; 25:251–262. [PubMed: 21245161]
18. Feng JH, Li WM, Wu XP, Tan XY, Gao YH, Han CL, Li SQ, Xie HN. Hemodynamic effect of apelin in a canine model of acute pulmonary thromboembolism. Peptides. 2010; 31:1772–1778. [PubMed: 20561551]
19. Frazier AA, Franks TJ, Mohammed T-LH, Ozbudak IH, Galvin JR. From the archives of the AFIP: pulmonary veno-occlusive disease and pulmonary capillary hemangiomatosis. Radio Graphics. 2007; 27:867–882.
20. Parker LH, Schmidt M, Jin SW, Gray AM, Beis D, Pham T, Frantz G, Palmieri S, Hillan K, Stainier DY, De Sauvage FJ, Ye W. The endothelial-cell derived secreted factor Egfl7 regulates vascular tube formation. Nature. 2004; 428:754–758. [PubMed: 15085134]
21. Nichol D, Shawber C, Fitch MJ, Bambino K, Sharma A, Kitajewski J, Stuhlmann H. Impaired angiogenesis and altered Notch signaling in mice overexpressing endothelial Egfl7. Blood. 2010; 116:6133–6143. [PubMed: 20947685]
22. Japp AG, Cruden NL, Amer DA, Li VK, Goudie EB, Johnston NR, Sharma S, Neilson I, Webb DJ, Megson IL, Flapan AD, Newby DE. Vascular effects of apelin in vivo in man. J Am Coll Cardiol. 2008; 52:908–913. [PubMed: 18772060]
23. Chun HJ, Ali ZA, Kojima Y, Kundu RK, Sheikh AY, Agrawal R, Zheng L, Leeper NJ, Pearl NE, Patterson AJ, Anderson JP, Tsao PS, Lenardo MJ, Ashley EA, Quertermous T. Apelin signaling antagonizes Ang II effects in mouse models of atherosclerosis. J Clin Invest. 2008; 118:3343–3354. [PubMed: 18769630]
24. Alastalo TP, Li M, de Perez VJ, Pham D, Sawada H, Wang JK, Koskenvuo M, Wang L, Freeman BA, Chang HY, Rabinovitch M. Disruption of PPARγ/β-catenin-mediated regulation of apelin impairs BMP-induced mouse and human pulmonary arterial endothelial survival. J Clin Invest. 2011; 121:3735–3746. [PubMed: 21821917]

25. Charo DN, Ho M, Fajardo G, Kawana M, Kundu RK, Sheikh AY, Finsterbach TP, Leeper NJ, Ernst KV, Chen MM, Ho YD, Chun HJ, Bernstein D, Ashley EA, Quertermous T. Endogenous regulation of cardiovascular function by apelin-APJ. Am J Physiol Heart Circ Physiol. 2009; 297:H1904–1913. [PubMed: 19767528]

26. Scott IC, Masri B, D'Amico LA, Jin SW, Jungblut B, Wehman AM, Baier H, Audigier Y, Stanier DY. The g-protein coupled receptor agtrl 1b regulates early development of myocardial progenitors. Dev Cell. 2007; 12:403–413. [PubMed: 17336906]

27. Drake JI, Bogaard HJ, Mizuno S, Clifton B, Xie B, Gao Y, Dumur CI, Fawcett P, Voelkel NF, Natarajan R. Molecular signature of a right heart failure program in chronic severe pulmonary hypertension. Am J Respir Cell Mol Biol. 2011; 45:1239–1247. [PubMed: 21719795]

28. Falcao-Pires I, Goncalves N, Henriques-Coelho T, Moreira-Goncalves D, Roncon-Albuquerque R, Leite-Moreira AF. Apelin decreases myocardial injury and improves right ventricular function in monocrotaline-induced pulmonary hypertension. Am J Physiol Heart Circ Physiol. 2009; 296:H2007–2014. [PubMed: 19346461]

29. Eyries M, Montani D, Girerd B, Perret C, Leroy A, Lonjou C, Chelghoum N, Coulet F, Bonnet D, Dorfmuller P, Fadel E, Sitbon O, Simonneau G, Tregouet DA, Humbert M, Soubrier F. EIF2AK4 mutations cause pulmonary veno-occlusive disease, a recessive form of pulmonary hypertension. Nat Genet. 2014; 46:65–70. [PubMed: 24292273]

30. Best DH, Sumner KL, Austin ED, Chung WK, Brown LM, Borczuk AC, Rosenzweig EB, Bayrak-Toydemir P, Mao R, Cahill BC, Tazelaar HD, Leslie KO, Hemnes AR, Robbins IM, Elliott CG. EIF2AK4 mutations in pulmonary capillary hemangiomatosis. Chest. 2014; 145:231–236. [PubMed: 24135949]

31. Berlanga JJ, Santoyo J, De Haro C. Characterization of a mammalian homolog of the GCN2 eukaryotic initiation factor 2alpha kinase. Eur J Biochem. 1999; 265:754–762. [PubMed: 10504407]

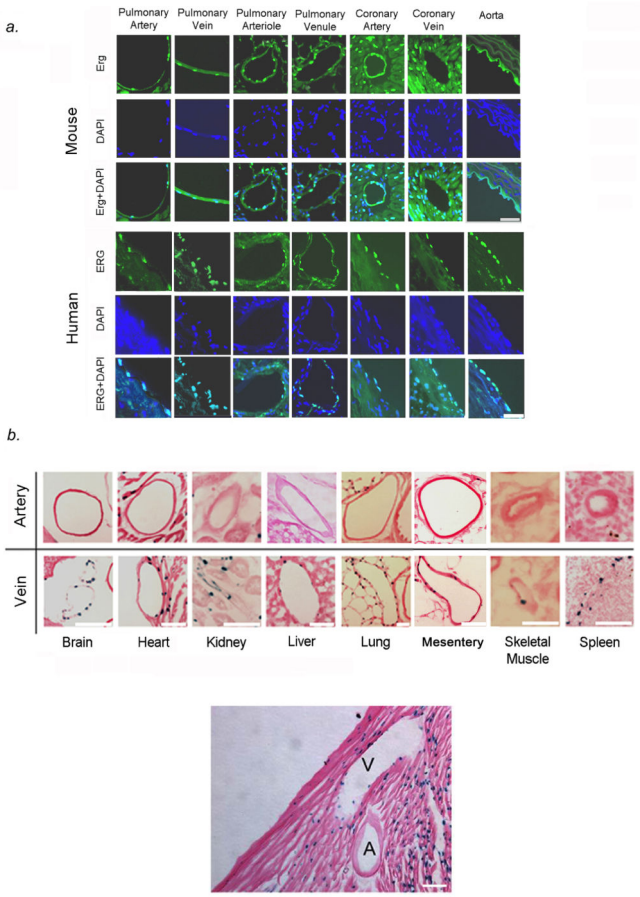

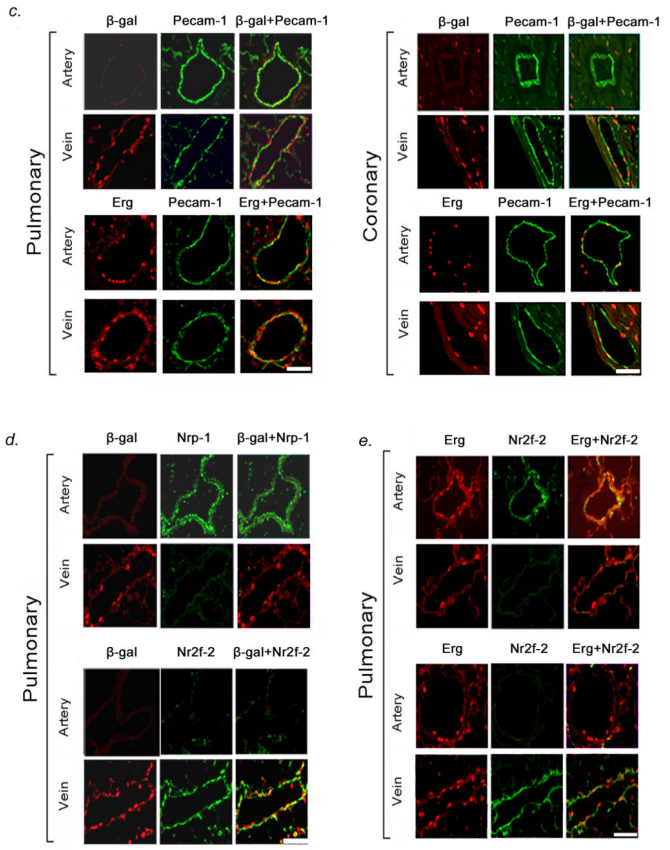

Figure 1.

Vascular specificity for Erg and Aplnr. (**A**) ERG (green) immunofluorescence staining in pulmonary vasculature, coronary circulation, and great vessels in mice (top panel) and humans (bottom panel), demonstrating specificity for both arteries and veins. Scale bars, 50μm. Results are representative sections from ten mouse hearts and lungs and ten human hearts and lungs. (**B**) Top panel: X-gal staining in *Aplnr*$^{-/-}$*:nlacZ* mouse tissues from 2-month old animals, showing venous specificity for Aplnr in multiple organs. Bottom panel: X-gal staining in *Aplnr*$^{-/-}$*:nlacZ* mouse heart showing Aplnr expression in coronary vein and myocardium, but not in coronary artery (A: artery, V: vein). Scale bar, 75μm. (**C**) Erg and Aplnr are specific to endothelium within pulmonary vessels, with Aplnr specific to venous endothelium. Top panel: β-gal (red) and Pecam-1 (green) immunofluorescence staining of *Aplnr*$^{-/-}$*:nlacZ* mouse pulmonary and coronary endothelium from 2-month old animals. Bottom panel: Erg (red) and Pecam-1 (green) immunofluorescence staining in the same tissues. Scale bars, 50μm. (**D**) Aplnr expression shows venous-endothelial specificity. β-gal (red) immunofluorescence staining with Nrp-1 (artery-specific, green: top panel) or Nr2f-2 (vein-specific, green: bottom panel) in pulmonary endothelium from 2-month old *Aplnr*$^{-/-}$*:nlacZ* mice, demonstrating venous specificity for Aplnr. Scale bars, 50μm. (**E**) Erg (red) and Nrp-1 (green: top panel) or Nr2f-2 (green: bottom panel) immunofluorescence staining of the same tissues in (D). Scale bars, 50μm. For (B) through (E), results are representative of ten sections per organ from at least ten mice per group.

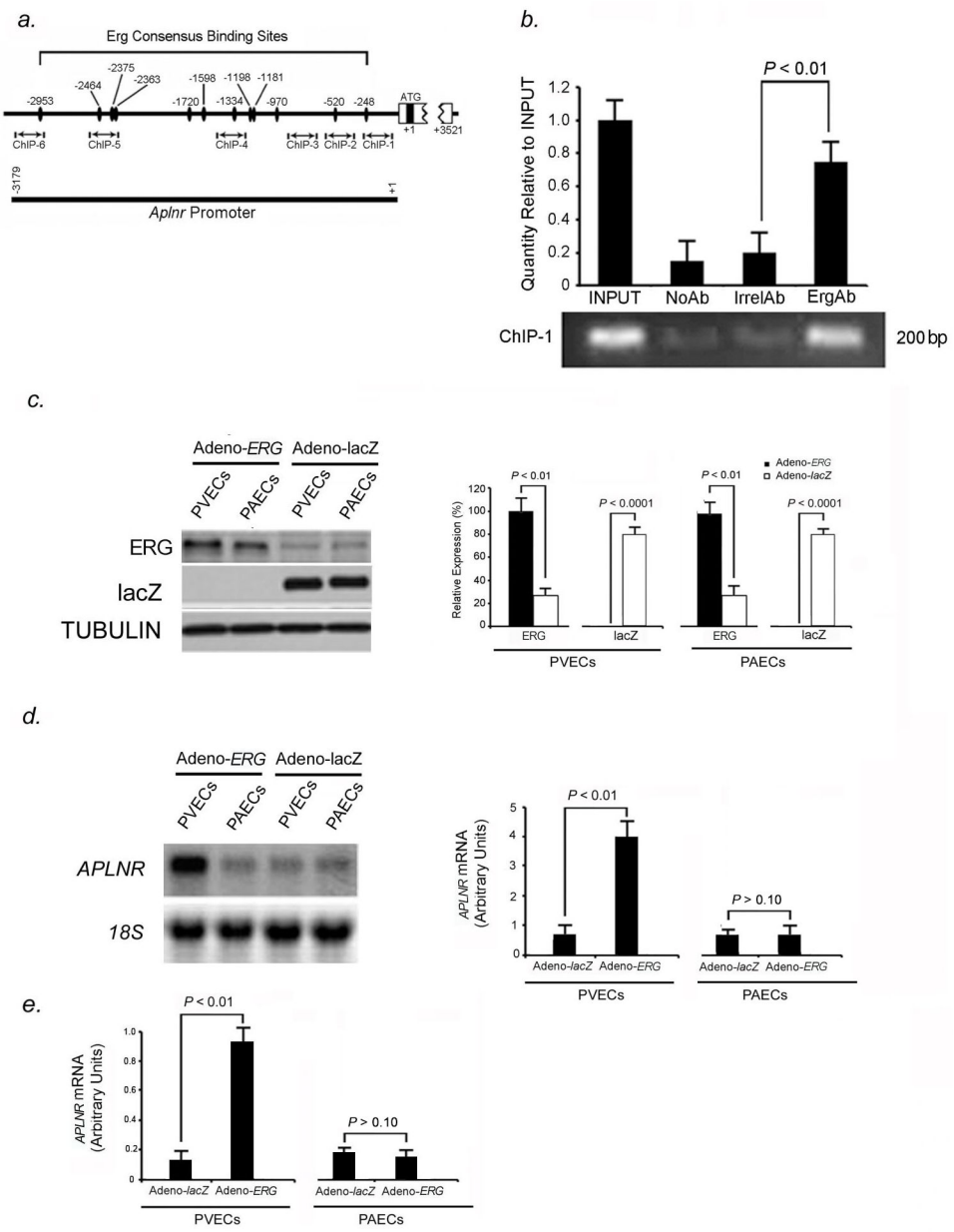

f.

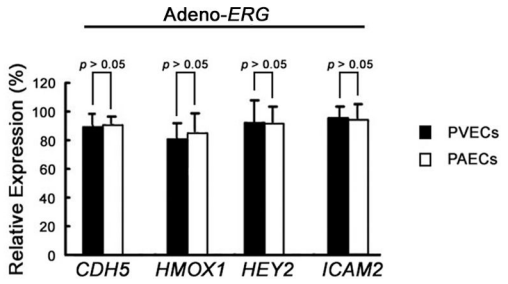

g.

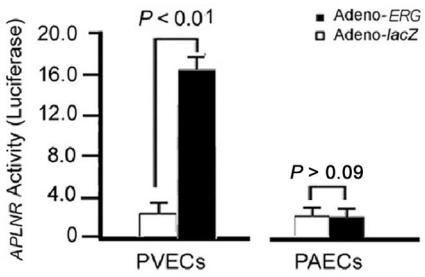

h.

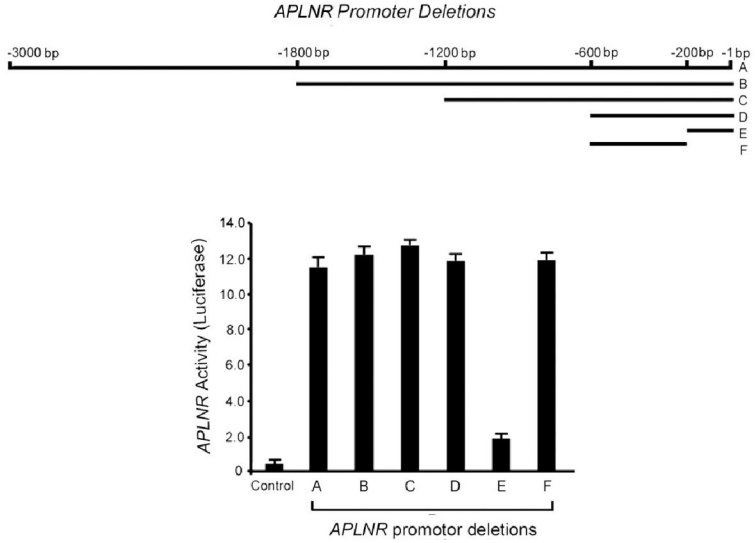

i.

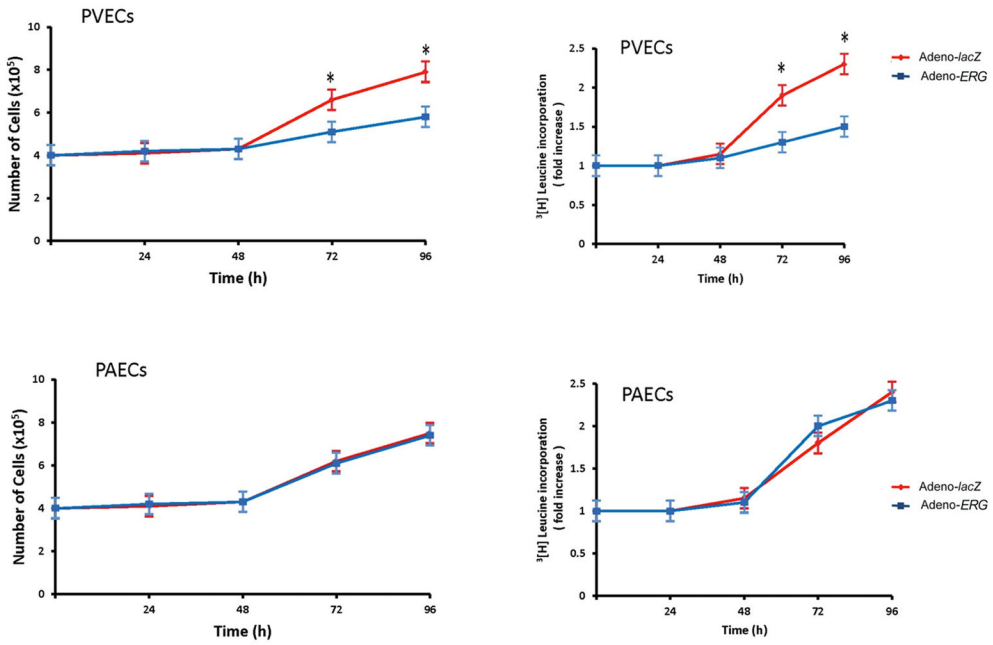

Figure 2.

Aplnr is a downstream target of Erg in PVECs. (**A**) Schematic diagram showing putative Erg binding sites in the mouse *Aplnr* promoter. The bidirectional arrows mark the target regions for ChIP assays. (**B**) Endogenous Erg binds to the *Aplnr* promoter. The experiment is representative of a set of four performed in triplicate in similar conditions. INPUT, total DNA; No Ab, no antibody added; Irrel Ab, irrelevant IgG added; ErgAb, antibody specific to Erg added. (**C**) Left, western blot analysis of ERG expression in human PVEC and PAEC subcultures infected with adenovirus containing the cDNA for *ERG* compared to the same subcultures transduced with *lacZ*-adenovirus. Right, relative expression value obtained by densitometry of ERG protein normalized to TUBULIN (n=3 PVEC cultures and 3 PAEC cultures, 3 transfections per culture, per group). (**D**) Left, northern blot analysis of *APLNR* expression in the same PVEC and PAEC subcultures as in (C), demonstrating increased *APLNR* expression only in PVECs overexpressing *ERG*. Right, relative expression value obtained by densitometry of *APLNR* mRNA normalized to *18S* rRNA (n=3 PVEC cultures and 3 PAEC cultures, 3 transfections per culture, per group). (**E**) qRT-PCR analysis confirming *APLNR* expression in the same PVEC and PAEC subcultures as in (C, D). (**F**) qRT-PCR analysis of genes, modulated by ERG, showing no difference between levels in PVEC and PAEC subcultures transduced with Adeno-*ERG*. (G) Overexpression of ERG induces *APLNR* transcriptional activity in PVECs as assessed by an *APLNR*-driven dual-reporter luciferase assay. (**H**) Top panel: Deletions in the *APLNR* promoter region tested in *APLNR*-luciferase activity (10 assays per group). Bottom panel: Region −200 to −600 base pairs 5′ of the *APLNR* start site is required for effective transcription of *APLNR*, as assessed by an *APLNR*-driven dual-reporter luciferase assay. (**I**) Left, growth curve of human PVECs and PAECs (n=10 PVEC cultures per group or 10 PAEC cultures per group) infected with adenovirus containing the cDNA for *ERG* compared to the same subcultures infected with

lacZ adenovirus. Right, ^{3}[H]leucine incorporation for the same cell samples. Overexpression of ERG slows the proliferative rate of PVECs, but not PAECs. **P*<0.01 compared to control group. Data are expressed as means ± s.e.m.

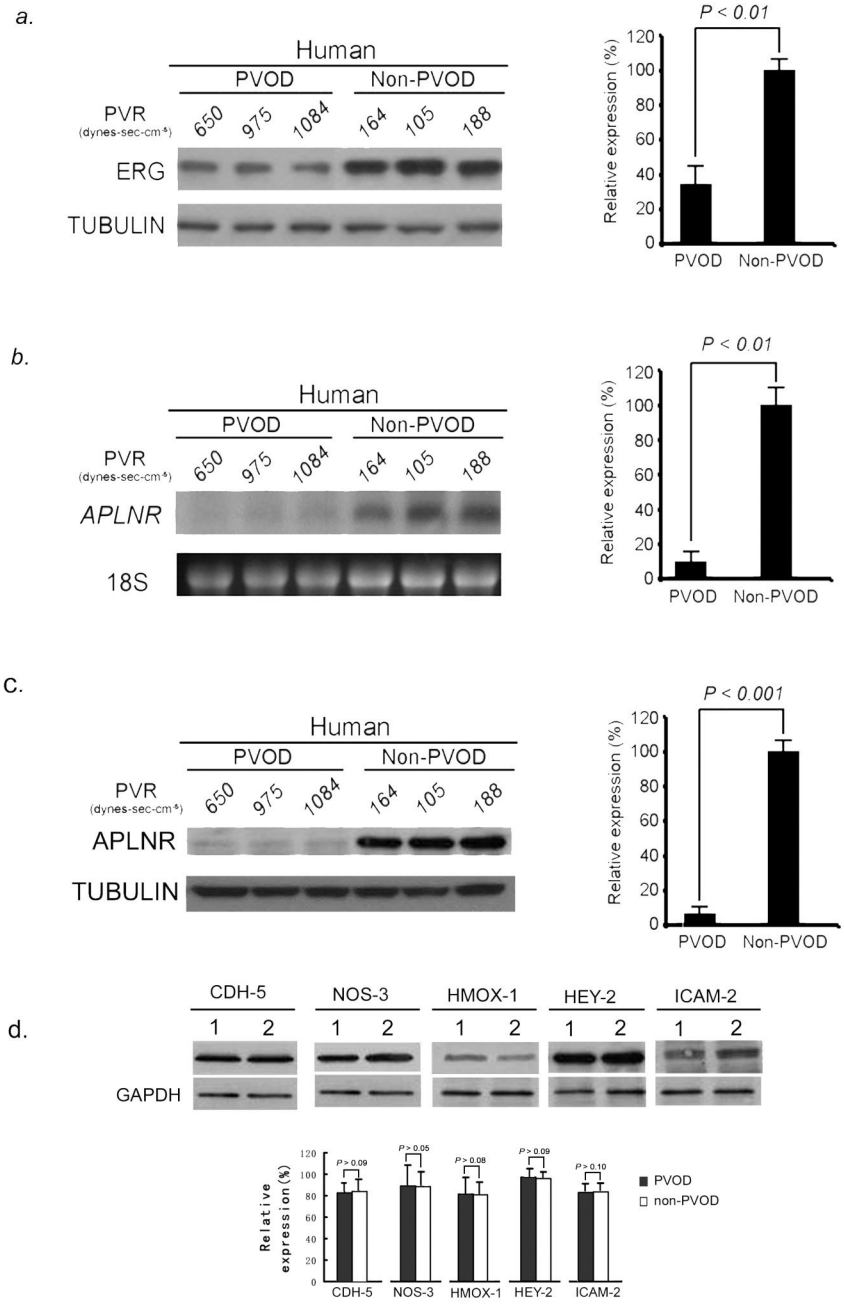

Figure 3.

Attenuation of ERG and APLNR expression in human PVOD lung tissue. (**A**) Left, western blot analysis of ERG relative to TUBULIN from human lungs with and without PVOD shows decreased levels of ERG in PVOD lung samples compared to controls (three representative PVOD subjects and three non-PVOD control subjects, shown of 15 analyzed for each group). Right, relative expression values obtained by densitometry of ERG protein normalized to TUBULIN (n=15 for each group). (**B**) Left, northern blot analysis of *APLNR* relative to *18S* rRNA from human lungs with and without PVOD demonstrating decreased levels of *APLNR* mRNA in PVOD lung samples compared to controls (three representative

PVOD subjects and three control subjects, shown of 15 analyzed for each group). Right, relative expression values obtained by densitometry of *APLNR* mRNA normalized to *18S* rRNA (n=15 for each group). (**C**) Left, western blot analysis of APLNR relative to TUBULIN from human lungs with and without PVOD shows decreased levels of APLNR protein in PVOD lung samples compared to controls (three representative PVOD subjects and three control subjects, shown of 15 analyzed for each group). Right, relative expression values obtained by densitometry of APLNR protein normalized to TUBULIN (n=15 for each group). (**D**) Top, western blot analysis of CDH-5, NOS-3, HMOX-1, HEY-2 and ICAM-2 proteins relative to GAPDH from human lungs with and without PVOD (single representative PVOD subject and non-PVOD subject, shown of 10 analyzed for each group; 1=PVOD lung tissue, 2=non-PVOD lung tissue), showing no difference in expression levels of these proteins in PVOD and normotensive human lung tissue. Bottom, relative expression values obtained by densitometry of each protein normalized to GAPDH (n=10 for each group). Data are expressed as means ± s.e.m.

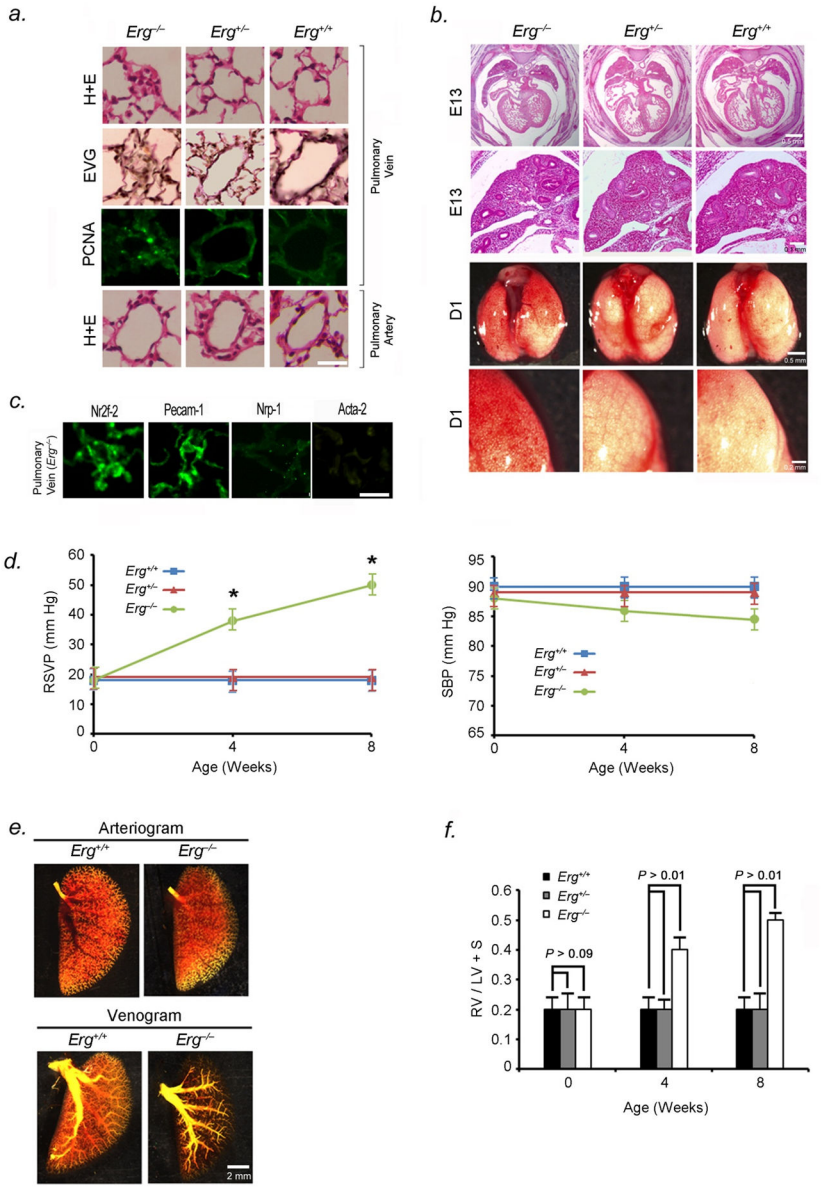

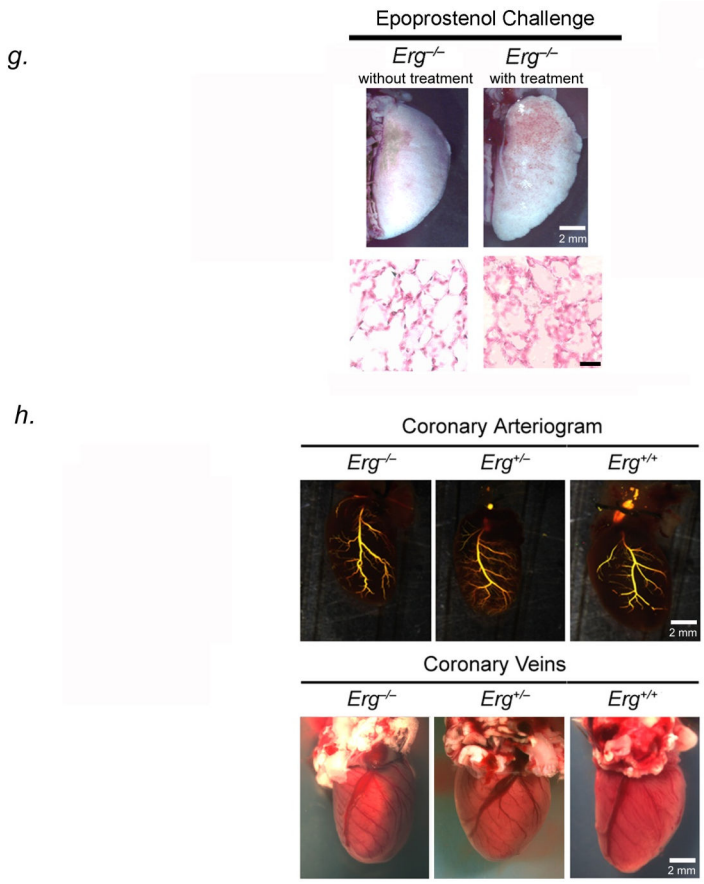

Figure 4.

$Erg^{-/-}$ mice develop PVOD and areas of pulmonary hemorrhage. (**A**) H&E-stained sections (row 1), EVG-stained sections (row 2), and immunohistochemical analysis of PCNA (row 3) of small pulmonary venules of 4 to 8-week old $Erg^{-/-}$, $Erg^{+/-}$, and $Erg^{-/-}$ mice, showing occlusion of venules < 250μm in diameter. Green nuclei are PCNA positive. Row 4 shows H & E-stained sections of small pulmonary arteries from the same animals. Results are representative sections from at least 15 mice per group. Scale bar, 50μm. (**B**) Top two panels, Whole mount H&E-stained sections of heart and lungs in $Erg^{-/-}$, $Erg^{+/-}$, and $Erg^{+/+}$ mice, showing normal lobar structure of the lung and normal right ventricular size and in knockout and heterozygous mice *in utero*. Bottom two panels, gross appearance of $Erg^{-/-}$, $Erg^{+/-}$, and $Erg^{+/+}$ mice lungs one day after birth, demonstrating hemorrhage in null mouse lungs. Results are representative of at least 20 mice per group, although hemorrhage is variable and more patchy in $Erg^{-/-}$ mice surviving after birth. (**C**) Immunofluorescence staining of occluded pulmonary vessels from 4 to 8-week old $Erg^{-/-}$ mice with antibodies to Pecam-1, Nr2f-2, Npr-1, and Acta-2, shows that the vessels are venules occluded by endothelial cells. Scale bar, 50μm. Results are representative sections from 20 mice. (**D**) $Erg^{-/-}$ mice develop pulmonary hypertension from PVOD. Averaged RVSP (left) and SBP (right) in $Erg^{-/-}$, $Erg^{+/-}$, and $Erg^{+/+}$ littermates surviving to 8 weeks of age (ten readings per mouse, ten mice per group at each timepoint). **P*<0.01 versus heterozygous and wildtype controls. (**E**) Pulmonary arterial (top) and venous (bottom)

angiograms of the left upper lobe of *Erg*$^{-/-}$ and *Erg*$^{+/+}$ mice. Venous angiograms from *Erg* null mice show severe vessel pruning and absence of contrast in small peripheral veins. Results are representative angiograms of ten mice, ranging from 2–4 weeks of age for each group. (**F**) *Erg*$^{-/-}$ mice develop right ventricular hypertrophy shortly after birth. Ratio of the weight of right ventricle (RV) to that of left ventricle plus septum (LV + S), as an index of RV hypertrophy in *Erg*$^{-/-}$ mice surviving to 8 weeks, compared to littermate controls (n=10 mice per timepoint for each group). (**G**) Photographs of left upper lobes (top panel) and representative H & E-stained sections (bottom panel) of 4-week old Erg$^{-/-}$ mice following 5-minute epoprostenol infusion (4 ng-kg^{-1}-min^{-1}), demonstrating severe pulmonary edema, with fluid in the intralveolar spaces (n=5 animals per group, 20 sections per animal examined), scale bar, 50μm. (**H**) Coronary arteriogram (top) and photographs of coronary veins (bottom) of 4-week old *Erg*$^{-/-}$, *Erg*$^{+/-}$, and *Erg*$^{+/+}$ mice. Results are representative of ten mice for each group. Data are expressed as means ± s.e.m.

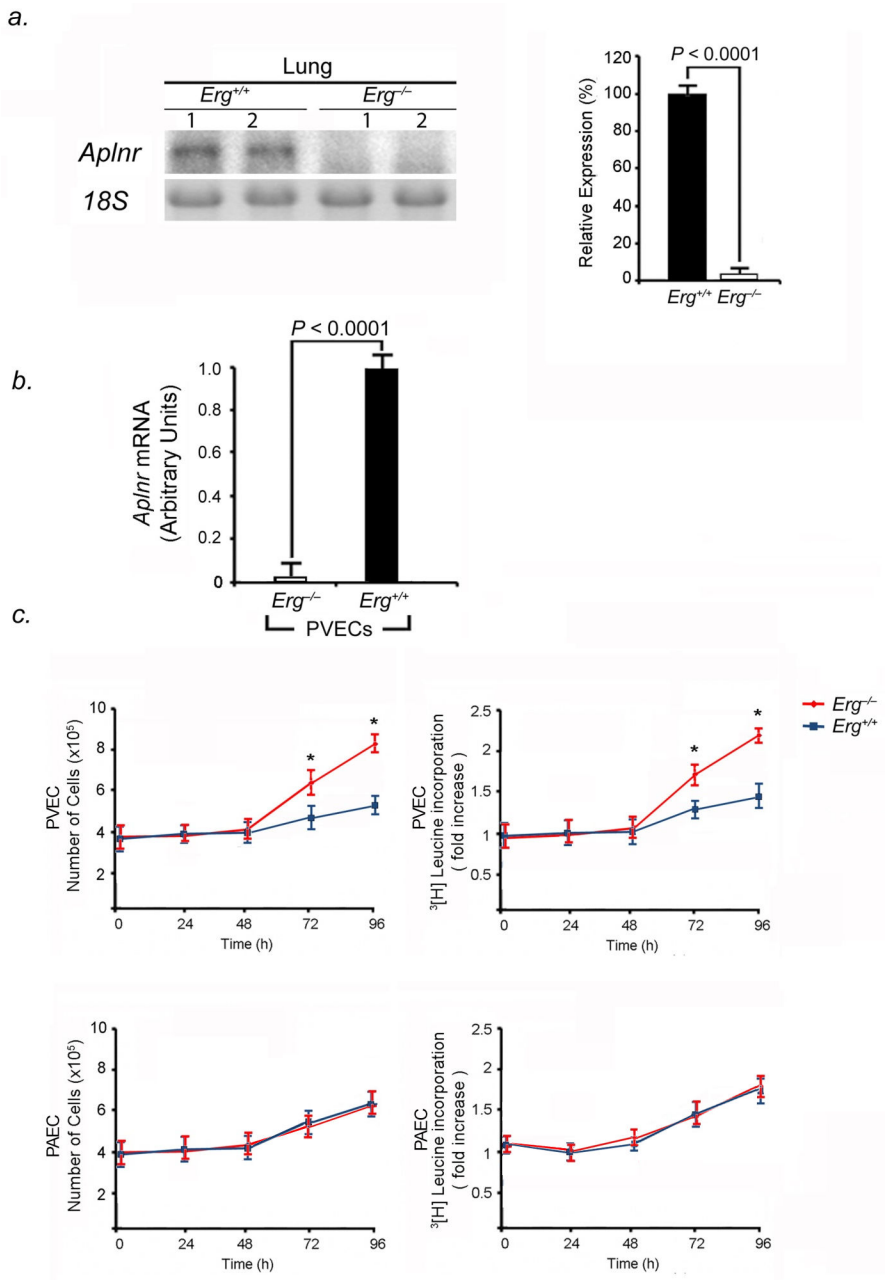

d.

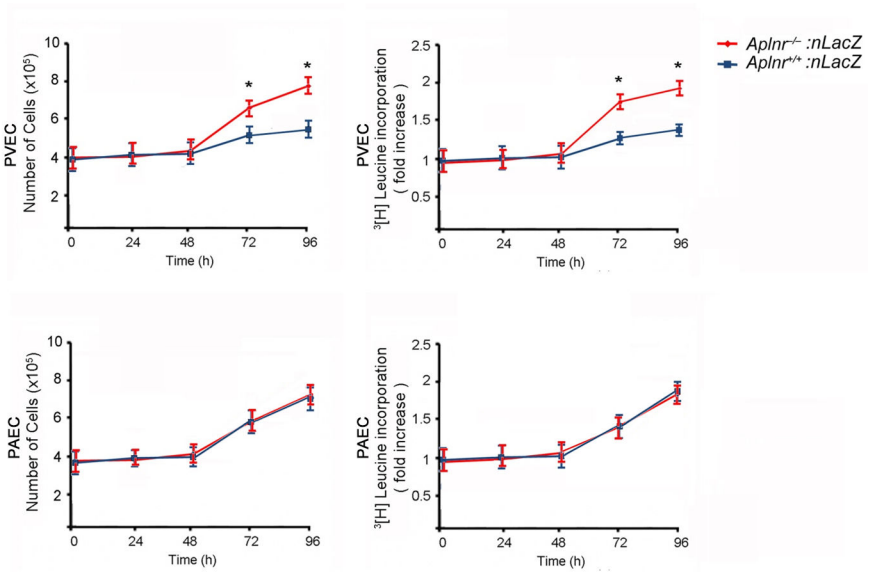

e.

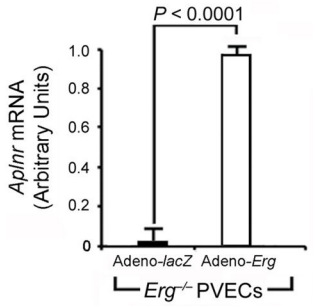

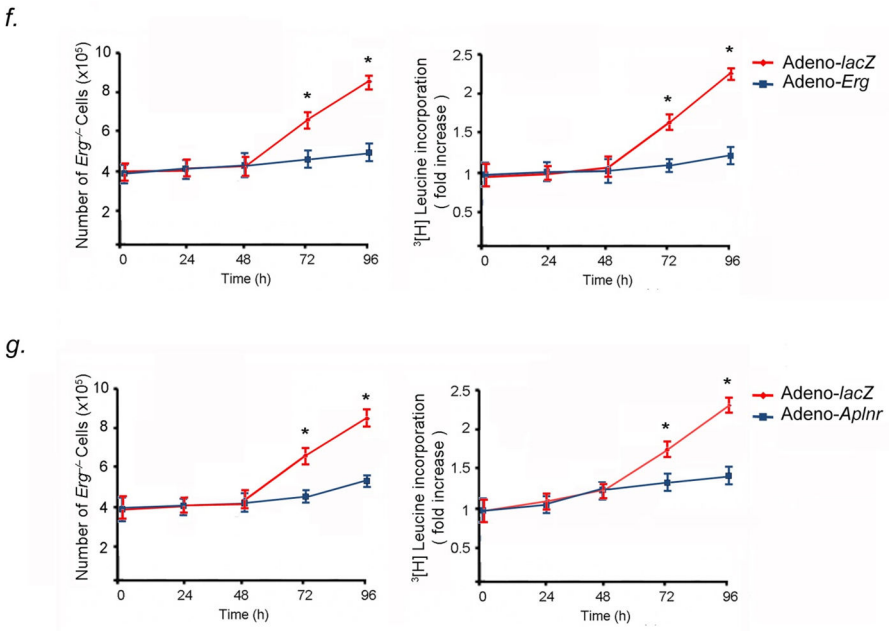

Figure 5.

Erg knockout increases PVEC proliferative capacity *in vitro*. (**A**) $Erg^{-/-}$ mice have undetectable levels of *Aplnr* mRNA in the lung. Left, northern blot analysis of *Aplnr* expression in the lungs of $Erg^{-/-}$ and $Erg^{+/+}$ 4-week old mice. Right, relative expression values obtained by densitometry of *Aplnr* mRNA normalized to *18S* rRNA in ten mice for each group. (**B**) $Erg^{-/-}$ PVECs have undetectable *Aplnr* mRNA levels compared to $Erg^{+/+}$ PVECs by qRT-PCR (n=5 animals per group, one subculture per mouse lung). (**C**) $Erg^{-/-}$ PVECs show higher proliferative rate than wildtype PVECs. Left, growth curve of PVECs and PAECs from $Erg^{-/-}$ and $Erg^{+/+}$ lungs (n=5 animals per group, one PVEC and one PAEC subculture per mouse lung). Right, ^{3}[H]leucine incorporation from the same cell samples. **P*<0.01 compared to wildtype. (**D**) $Aplnr^{-/-}$:nlacZ PVECs show higher proliferative rate than wildtype PVECs. Left, growth curve of PVECs and PAECs from $Aplnr^{-/-}$:nlacZ and $Aplnr^{+/+}$:nlacZ lungs (n=5 animals per group, one PVEC and one PAEC subculture per mouse lung). Right, ^{3}[H]leucine incorporation for the same cell samples. **P*<0.01 compared to wildtype. (**E**) Induced expression of *Erg* restores *Aplnr* expression in $Erg^{-/-}$ PVECs as measured by qRT-PCR. (n=5 animals per group, one subculture per mouse lung). Cells were transduced with adenovirus containing the cDNA for *Erg* compared to the same subcultures transduced with *lacZ*-adenovirus. (**F**) Restoration of *Erg* expression slows proliferation of $Erg^{-/-}$ PVECs. Left, growth curve of PVECs from $Erg^{-/-}$ mice (n=5 per group, one subculture per mouse lung) transduced with either *Erg*-adenovirus or *lacZ*-adenovirus. Right, ^{3}[H]leucine incorporation for the same cell samples. **P*<0.01 compared to control groups. (**G**) Expression of *Aplnr* slows proliferation of $Erg^{-/-}$ PVECs. Left, growth curve of PVECs from $Erg^{-/-}$ mice (n=5 per group, one subculture per mouse lung) transduced with either *Aplnr*-adenovirus or *lacZ*-adenovirus. Right, ^{3}[H]leucine incorporation for the same cell samples. **P*<0.01 compared to control groups. Data are expressed as means ± s.e.m.

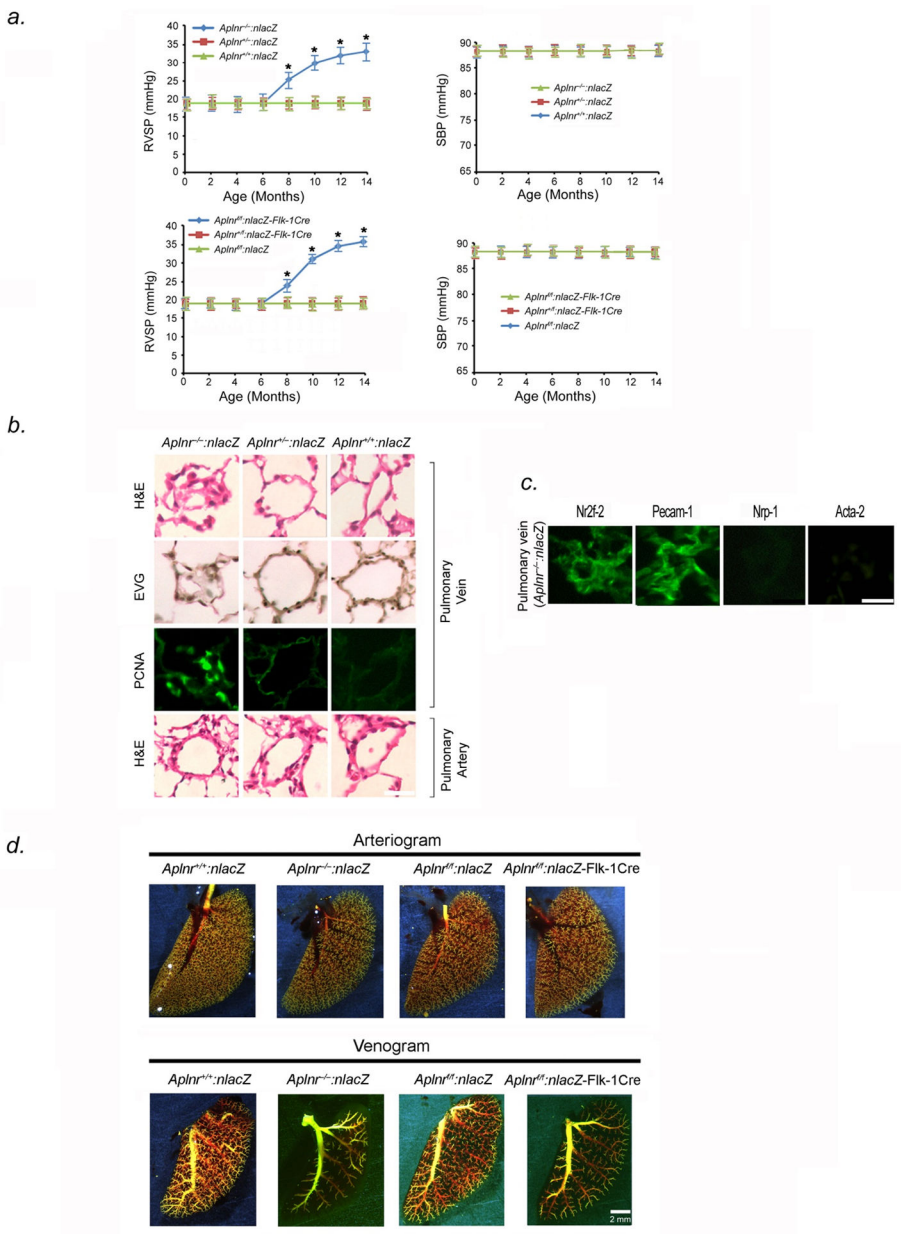

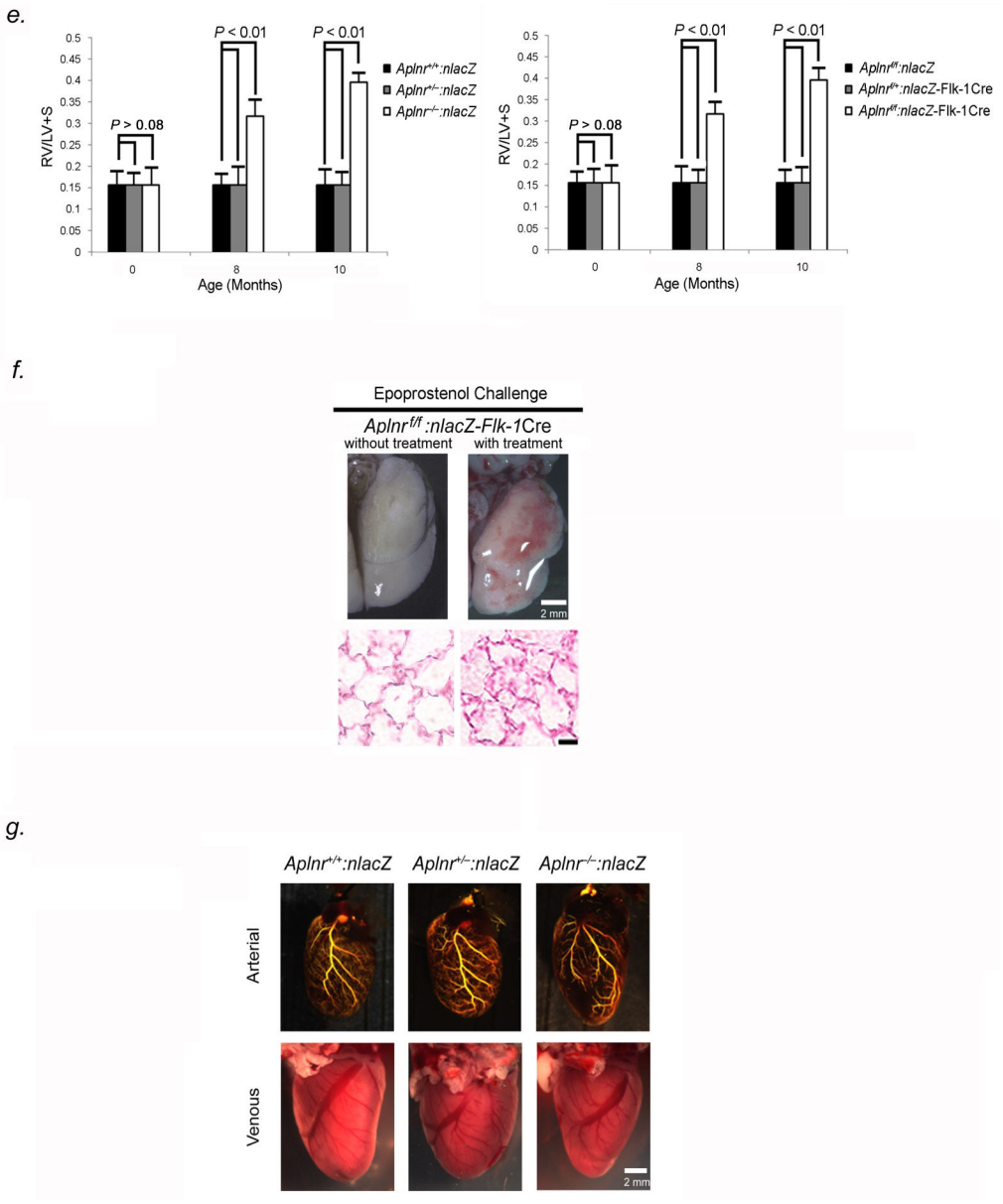

Figure 6.

Aplnr$^{-/-}$*:nlacZ* and *Aplnr*$^{f/f}$*:nlacZ*-Flk-1Cre mice develop PVOD by 8 months of age. (**A**) Averaged RVSP (left) and SBP (right) in *Aplnr*$^{-/-}$*:nlacZ*, *Aplnr*$^{+/-}$*:nlacZ*, *Aplnr*$^{+/+}$*:nlacZ* mice as well as in *Aplnr*$^{f/f}$*:nlacZ*-Flk-1Cre, *Aplnr*$^{f/+}$*:nlacZ*-Flk-1Cre, and *Aplnr*$^{f/f}$*:nlacZ* mice up to 14 months of age (ten readings per mouse, ten mice per group). **P*<0.01 versus controls. (**B**) H & E-stained sections (row 1), EVG-stained sections (row 2), and immunohistochemical analysis of PCNA (row 3) of small pulmonary venules from lungs of 8-month old *Aplnr*$^{-/-}$*:nlacZ*, *Aplnr*$^{+/-}$*:nlacZ* and *Aplnr*$^{+/+}$*:nlacZ* mice, showing severe narrowing/occlusion of venules <250μm in diameter. Green nuclei are PCNA positive. Row 4 shows H & E-stained sections of small pulmonary arteries from the same animals. Results are representative sections from at least 15 mice per group. Scale bar, 50μm. (**C**) Immunofluorescence staining of occluded pulmonary venules from 8-month old *Aplnr*$^{-/-}$

mice with antibodies to Nr2f-2, Pecam-1, Nrp-1, and Acta-2, shows that the vessels are stenotic venules blocked by endothelial cells. Scale bar, 50μm. Results are representative sections from 15 mice. (**D**) Pulmonary arterial (top) and venous (bottom) angiograms of 10-month old *Aplnr*$^{-/-}$*:nlacZ* and *Aplnr*$^{f/f}$*:nlacZ*-Flk-1Cre mice compared to wildtype controls. Venous angiograms from *Aplnr* null mice show severe vessel pruning and absence of contrast in small peripheral veins. Results are representative angiograms of ten mice for each group. (**E**) *Aplnr*$^{-/-}$ mice develop right ventricular hypertrophy by 8 months of age. Ratio of the weight of RV to that of LV + S, as an index of RV hypertrophy in 8 and 10-month *Aplnr*$^{-/-}$*:nlacZ* (left panel) and *Aplnr*$^{f/f}$*:nlacZ*-Flk-1Cre mice (right panel), compared to age-matched controls (n=10 mice per timepoint for each group). (**F**) Representative photographs of gross lung tissue (top panel) and H & E-stained sections (bottom panel) of 10-month old *Aplnr*$^{f/f}$*:nlacZ*-Flk-1Cre, following 5-minute epoprostenol infusion (4 ng-kg^{-1}-min^{-1}). (n=5 animals per group), Scale bar, 50μm. (**G**) Coronary arteriograms (top) and photographs of coronary veins (bottom) of 10-month old *Aplnr*$^{-/-}$*:nlacZ*, *Aplnr*$^{+/-}$*:nlacZ*, and *Aplnr*$^{+/+}$*:nlacZ* mice. Results are representative angiograms of ten mice for each group.